Int. J. Electrochem. Sci., 14 **(2019)** 705 – 716, doi: 10.20964/2019.01.34

International Journal of
ELECTROCHEMICAL
SCIENCE
www.electrochemsci.org

The Electrochemical Performances of Zn-Al-Hydrotalcites in Zn-Ni Secondary Batteries

Xiaohua Yu[1], *Yasong Qu*[1],*Shuanglin Yu*[1],*Yunting Cai*[1], *Xiaocai He*[2], *Pan Feng*[1], *Ying Wang*[1] *Gang Xie*[1,3]

[1] Faculty of metallurgy and energy engineering, Kunming University of Science and Technology, Kunming Yunnan 650093, China
[2] Yunnan Metallurgical Group Chuang Neng Metal fuel battery Co., LTD, Kunming 650503, China
[3] State key laboratory of pressure hydrometallurgical technology of associated non-ferrous metal resources, Kunming Yunnan 650503, China
[*]E-mail: yxhyxh1978@aliyun.com

Received: 14 September 2018 / *Accepted:* 5 November 2018 / *Published:* 30 November 2018

Zn-Al-hydrotalcites (Zn-Al-LDHs) are successfully synthesized by a hydrothermal method and a co-precipitation method and are investigated as negative electrode materials for Zn-Ni batteries. Scanning electron microscope (SEM) images, X-ray diffraction (XRD) patterns and laser scattering particle analysis show that the as-prepared sample is flaky in structure and well-crystallized, and the particle sizes are approximately 20-40 μm. The electrochemical performances of Zn-Al-LDHs determined by different methods are investigated by potentiodynamic polarization, electrochemical impedance spectroscopy (EIS) and galvanostatic charge/discharge measurements. Compared with pure ZnO powders, Zn-Al-LDHs have good anticorrosion ability. The lower charge platform (1.86 V) and higher discharge platform (1.71 V) of Zn-Al-LDHs indicate that they have better charge/discharge performance as negative active materials for Zn-Ni batteries. These findings show excellent cycle stability in the 40th cycle, with the capacity retention ratio of 81.4% and cycle effciency of approximately 90%, which are much higher than those of pure ZnO (44%).

Keywords: Zn-Al-LDHs; Zn-Ni secondary batteries; Electrode performance; Cyclic stability

1. INTRODUCTION

In recent years, Zn-Ni secondary batteries, with high specific energy (50~80 $Wh \cdot kg^{-1}$), high specific power (500 $W \cdot kg^{-1}$), high working voltage (1.2~1.5 V), high operating voltage (1.75 V), and no memory effect, have attracted much attention. However, Zn-Ni batteries are usually limited in widespread commercialization by the drawbacks of zinc electrodes, such as zinc dendrites, passivation,

zinc self-corrosion and shape changes in the charge-discharge process. The problems mainly derive from the high solubility of zinc active materials in alkaline electrolytes [1, 2]. Upon charging, zinc ions can deposit on the surface of the zinc electrode, which leads to a zinc electrode surface that is not uniform[3].

Hence, many attempts have been made to overcome these problems, and most researchers have focused on the negative material to solve the drawbacks and enhance the cycle life of zinc electrodes. For example, Huang[4] put a layer of carbon on the surface of Zinc Oxide., and the researchers found that the cycle life of the zinc negative electrode was improved. Xu [5] analysed $In(OH)_3$ coated onto the surface of ZnO by a co-precipitation method, which improved the corrosion resistance of ZnO and enhanced the cycle life of the battery. Yano [6] used a dry-coating process to prepare a zinc alloy that contained In, Bi and Pb to improve the stability of zinc oxide powder, and hydrogen-gas evolution is suppressed effectively. Palagyi [7] found that adding LiOH to the electrolyte can effectively prevent the decomposition of zincate, thereby slowing the passivation of the zinc electrode . Han[8] used ultrasonic-assisted polymerization to synthesize ZnO/polypyrrole composites for zinc/nickel rechargeable batteries, which significantly improved their performance. Yang [9] synthesized $Ca(OH)_2$ and ZnO as new substances through a chemical precipitation method to increase the corrosion resistance of the zinc electrode and improve the cycle life of the zinc electrode. At present, calcium zincate synthesized from $Ca(OH)_2$ and ZnO is the most effective material to solve these problems. But calcium zincate has poor performance in conductivity and low specific capacity; meanwhile, the synthesis process is complex and has a higher production cost [10, 11, 16]. To ameliorate the defects of calcium zincate, researchers found that compounds of Zn and Al can be synthesized into Zn-Al-hydrotalcites (Zn-Al-LDHs) [12-14], which have similar advantages to those of Mg-Al-hydrotalcites[18,19] and overcome the defects of calcium zincate. Fan [15] found that Zn-Al-LDHs can enhance the cycle life of zinc negative electrodes. Among these studies, the use of Zn-Al-LDHs as negative electrodes is the most effective solution.

In this work, we emphasize preparation of Zn-Al-LDHs by a simple hydrothermal method and a co-precipitation method. The effects of Zn-Al-LDHs prepared by the two different methods are compared with that of pure ZnO in terms of structure and electrochemical performance, and Zn-Al-LDHs are investigated in detail as negative materials in Zn-Ni secondary batteries.

2. EXPERIMENTAL

2.1 The preparation of Zn-Al-LDHs

Zn-Al-LDHs were prepared via a simple co-precipitation method and a hydrothermal method. The typical experimental operation was as follows. According to the molar ratio of 3:1, certain amounts of zinc nitrate hexahydrate and aluminium nitrate hexahydrate were prepared, and a salt solution of $[Zn^{2+}]$=0.3 mol/L was prepared. The salt solution was put into ultrasonicated waves for 15 min, so that the salt solution was evenly mixed. Then, according to the molar ratios of n (CO_3^{2-}) / n (Al^{3+}) = 2 and n (NaOH) / n $(Zn^{2+} + Al^{3+})$ = 2, a mixed salt of sodium hydroxide and sodium carbonate was prepared. A solution of 500 mL was added, to which 1% PE2000 was also added, and the salt solution was fully mixed by ultrasonication for 10~20 min, after which the solution was well-distributed. The two saline

solutions described above were added simultaneously into a three-necked flask at a speed of 1 drop s^{-1} through a peristaltic pump under constant mechanical stirring, and by maintaining $n(CO_3^{2-})/n(Al^{3+})=2$, $n(NaOH)/n(Zn^{2+}+Al^{3+})=2$ and pH=10, a white emulsion was obtained. Then, Zn-Al-LDHs were prepared by two different methods. For the hydrothermal method, the process was carried out under vigorous stirring at 85ºC, and after stirring for 4 h, the mixture was aged for 24 h at 65ºC. The product was filtered and washed several times with deionized water until the pH reached 7 at 70ºC, then dried for 24 h at 80ºC and ground to a fine powder. For the co-precipitation method, the white emulsion was aged for 2 h at 65ºC, then poured into autoclave and kept at 120ºC for 12 h. The product was cooled to 70ºC, filtered and washed several times with deionized water until the pH reached 7, then dried for 24 h at 80ºC and ground to a fine powder.

2.2 The preparation of Zn-Al-LDHs and pure-ZnO electrodes

The Zn-Al-LDHs or pure-ZnO electrodes were prepared by incorporating slurries containing 85 wt% Zn-Al-LDHs or pure ZnO, 6 wt% acetylene black, 4 wt% zinc powder, 5 wt% polytetrafluoroethylene (PTFE, in a diluted emulsion) and an appropriate amount of absolute ethyl alcohol. The resulting paste was filtered, pressed to a thickness of 0.30 mm and dried at 80ºC under vacuum. A copper mesh substrate (50 mm×60 mm) served as the current collector, and the electrodes were roll-pressed onto it.

2.3 The characterization of Zn-Al-LDHs

The as-prepared powder was then characterized by X-ray diffraction (XRD, FMPYREAN PANALYTICAL) using a D500 diffractometer (40 kV, 40 mA) with Cu Kα radiation (λ=0.154056 nm) at a scanning rate of $2\theta=8^{o}$ min^{-1} to obtain the crystalline structure and phase composition. The morphology of Zn-Al-LDHs was observed using a scanning electron microscope (SEM, KMRIWCS 3000). The particle size was obtained using a laser scattering particle analyser (Malvern 2000).

2.4. The measurements of electrochemical properties

The AC impedance spectroscopy analysis was carried out on a PGSTAT302N (Metrohm) electrochemical workstation at room temperature (25 ºC). A three-electrode cell assembly was used in the test, with a Hg/HgO electrode as the reference electrode, a commercial sintered $Ni(OH)_2$ electrode as the counter electrode, and a pre-activated zinc electrode as the working electrode (2.0×2.0 cm, thickness of 0.3 mm). The linear scan rate was set to 1 mV s^{-1}. The applied frequency range of EIS was between 0.01 Hz and 100 Hz, and the amplitude of the AC signal was set at 10 mV.

The galvanostatic charge/discharge cycling tests were performed using a CT2001A battery-testing instrument (LAND, China) at room temperature (25 ºC). The pre-activated zinc electrodes were pre-activated three times to reach the ideal discharging efficiency by the following operation: the batteries were charged at 0.1 C for 12 h, and after stewing, they were discharged for 5 min at 0.1 C down

to the 1.0 V cut-off. During the cycling process, the batteries were charged at 0.2 C for 6 h and discharged at 0.2 C to a cut-off voltage of 1.2 V in regular succession to test the performance of the zinc electrode. The electrolyte used was a solution of 6 mol·dm^{-3} KOH and 1 mol·dm^{-3} LiOH, saturated with ZnO.

3. RESULTS AND DISCUSSION

3.1. Structural analysis of Zn-Al-LDHs

Fig. 1 shows the XRD patterns of the as-prepared Zn-Al-LDHs powder (a: hydro-thermal method; b: co-precipitation method) for comparison. It can be clearly seen that the strong and sharp diffraction peaks of Zn-Al-LDHs at 2θ=11.77°, 23.43°, 34.66°, and 60.07° correspond to the structures of {002}, {004}, {426} and {110}, respectively, which can also be seen in the standard photographs of Zn-Al-LDHs. The diffraction peaks of the two different preparation methods are similar, which shows that Zn-Al-LDHs can be obtained by the two methods. The results are consistent with the XRD pattern of Zn-Al-LDHs reported in previous literature [13,17,20,21]. This indicates that zinc and aluminium hydrotalcites were prepared in this paper and other studies.The diffraction peaks of the hydrothermal method are sharper and higher than those of the co-precipitation method, which indicates that Zn-Al-LDHs obtained by the hydrothermal method are highly crystallized and have a good crystal structure.

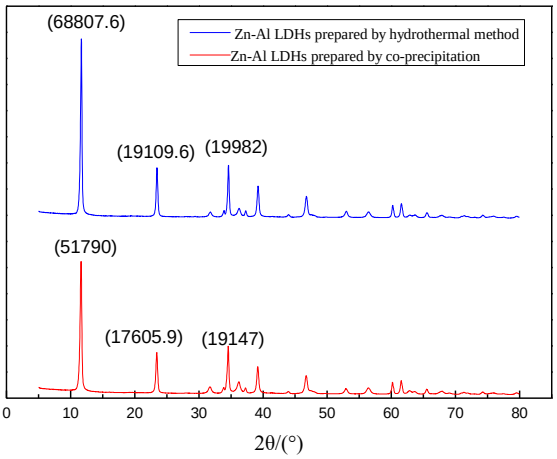

Figure 1. XRD patterns of Zn-Al-LDHs particles prepared by the hydrothermal method and the co-precipitation method (The parameters used were Cu target Kα radiation with a Cu filter, an acceleration voltage of 40 kV, a current of 40 mA, and a scanning speed of 8° min^{-1};)

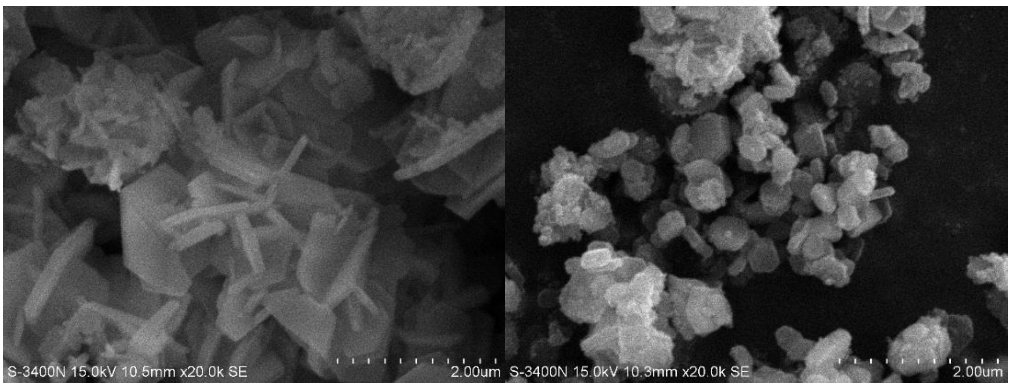

a b

Figure 2. SEM images of Zn-Al-LDHs particles (a: hydrothermal method, b: coprecipitation method) (Parameters: acceleration voltage of 35 KV and 25 KV, respectively, and test temperature at room temperature)

Fig. 2 (a-b) shows typical SEM images of Zn-Al-LDHs prepared by the hydro-thermal method and the co-precipitation method. It can be found that samples a and b have similar crystal hexagon layer structures. The surface of Zn-Al-LDHs prepared by the hydro-thermal method is smooth, with uniform dispersion and interspersed with hexagonal flakes, and the thickness of each piece is thinner than that of Zn-Al-LDHs prepared by co-precipitation. The agglomeration phenomenon of Zn-Al-LDHs prepared by co-precipitation is more serious.

Fig. 3 presents the particle size analysis patterns of Zn-Al-LDHs prepared by the two methods. It can be seen that the Zn-Al-LDH particle size patterns resulting from the two methods follow an evenly normal distribution, with d_{50}=12.47 μm, d_{90}=22.22 μm, and d_{95}=25.35 μm for the hydrothermal method and d_{50}=19.38 μm, d_{90}=33.97 μm, and d_{95}=38.38 μm for the co-precipitation method. Although the particles are not as fine as the nano-Zn-Al-LDH particles reported by Yang[14], they are finer than those of Zn-Al-LDHs prepared in other studies[17,21-23]. This is mainly because Yang added a nanocrystallization step for the zinc-aluminium hydrotalcite, so the zinc-aluminium hydrotalcite prepared herein does not have comparative fineness in terms of particle size. This illustrates that the hydrothermal method is a good method for the preparation of Zn-Al-LDHs, resulting in a fine and uniform particle size and conforming to the SEM analysis results, because the high temperature is good for the growth of crystalline Zn-Al-LDHs and can remove the agglomeration phenomenon caused by Na^+ to make the hydrothermal particles disperse evenly.

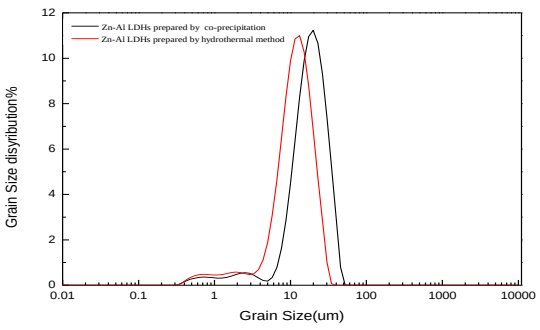

Figure 3. Particle size distribution of Zn-Al-LDHs prepared by the hydrothermal method and the co-precipitation method

3.2 The AC impedance spectroscopy analysis of Zn electrodes

Fig. 4 (a) shows the AC impedance diagram of the ZnO electrode and the Zn-Al-LDHs prepared by the two methods, and the corresponding electrochemical equivalent circuit is shown in Fig. 4 (b).

As shown in Fig. 4, the electrochemical impedance diagrams of the three kinds of negative electrode materials are approximately similar, both comprised of a high-frequency capacitive semicircular loop and a low-frequency straight line. The high-frequency capacitive semicircular loop can be ascribed to the charge-transfer resistance in parallel with the double-layer capacitance, and the slope of the low-frequency region is most likely caused by the Warburg diffusion impedance effect and the diffusion of zincate in the zinc electrode. Generally, the charge-transfer impedance (R_{ct}) increases with the capacitance radius, which leads to the electrochemical reaction becoming more difficult and the electrochemical polarization increasing. Fig. 4 (a) displays the charge-transfer impedance (R_{ct}) values of 21.8 Ω, 38.4 Ω and 57.1 Ω corresponding to the Zn-Al-LDHs and ZnO electrodes. It can be seen that the internal resistance of Zn-Al-LDHs is lower than that of ZnO, which illustrates that Zn-Al-LDHs more easily transfer electric charge and are faster to react compared with pure ZnO. Moreover, the resistance is lower than that of other zinc electrodes prepared by zinc oxide modification[11]. Compared with other hydrotalcite-like electrodes, the zinc-aluminium hydrotalcite electrode prepared in this paper has a relatively low Rct, which indicates that the conductivity of the zinc-aluminium hydrotalcite electrode prepared in this paper is superior to that of other hydrotalcite electrodes in other studies[17,20-23].Meanwhile, it can be clearly found that the Zn-Al-LDHs prepared by the hydrothermal method have a lower transfer resistance and better charge transfer capacity compared with those prepared by the co-precipitation method.

Table 1 shows the impedance spectrum data of the Zn-Al-LDHs and ZnO electrodes. The Rct values of the Zn-Al-LDHs (co-precipitation method), Zn-Al-LDHs (hydrothermal method) and ZnO electrodes were 0.25 Ω， 0.22 Ω and 0.36 Ω respectively. When the Rct is larger, the electrochemical reaction of the electrode is more difficult, and the electrochemical polarization of the electrode is more serious. Therefore, the electrochemical reaction of the Zn-Al-LDHs electrode is easier than that of the ZnO electrode, so its performance is better than that of the ZnO electrode.

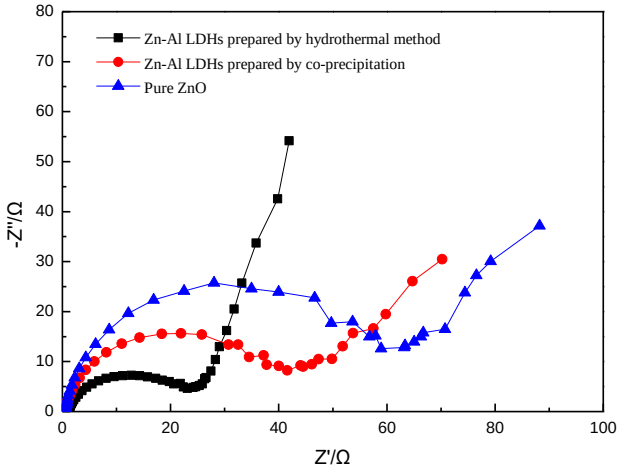

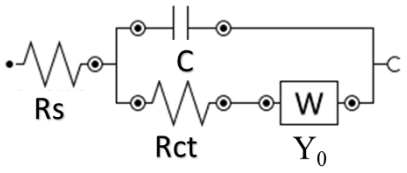

Figure 4. AC impedance diagrams and equivalent circuit diagram of Zn-Al-LDHs and pure ZnO (Parameters: frequency range of 0.01~10000 HZ and test temperature at room temperature)

Table 1. AC impedance test parameters of the Zn-Al-LDHs and zinc oxide electrodes

Sample name	R_s (Ω)	R_{ct} (Ω)
ZnO	1.01	0.36
Zn-Al-LDHs (co-precipitation method)	0.27	0.25
Zn-Al-LDHs (hydrothermal method)	0.24	0.22

3.3 Potentiodynamic polarization curves of zinc electrodes

Fig. 5 shows the corrosion resistance test results of the pure-ZnO electrode and the Zn-Al-LDHs electrodes. The electrochemical kinetic parameters derived from these curves are shown in Table 2.

Potentiodynamic polarization curves can be used to study the polarization characteristics of electrodes. Due to changes of the electrode potential, the characteristics of the double layer on the electrode surface are constantly changing, which leads to changes of the electrode process dynamics. As shown in Fig. 5, the potentiodynamic polarization curve of the Zn-Al-LDHs electrode is approximately the same as that of the pure-ZnO electrode. The polarization current increases with the increase of the polarization potential. The polarization current of the zinc oxide electrode is always higher than that of the Zn-Al-LDHs electrodes in this process, indicating that the Zn-Al-LDHs electrodes are more corrosion resistant. Zinc oxide and Zn-Al-LDHs (co-precipitation) have obvious peaks, but Zn-Al-LDHs prepared by the hydrothermal method have none, indicating that Zn-Al-LDHs (hydrothermal method) has better corrosion resistance. From Table 2, the corrosion current densities of pure ZnO and the Zn-Al-LDHs appear respectively at 3.998 $mA \cdot cm^{-2}$, 3.719 $mA \cdot cm^{-2}$ and 3.454 $mA \cdot cm^{-2}$. These data are superior to those reported in the literature because the corrosion current of some hydrotalcite electrodes prepared in previous studies exceeded 4 $mA \cdot cm^{-2}$ under the same conditions, so the Zn-Al-LDHs electrodes prepared in this paper are superior in terms of corrosion resistance[17,20-23].The corrosion current density (I_{corr}) is expressed as the corrosion rate of the zinc electrode. Generally, if the corrosion current density increases, the electrode is corroded faster. The results show that the corrosion resistance of the Zn-Al-LDHs is better than that of pure ZnO, and the Zn-Al-LDHs prepared by the hydrothermal method is better than that of Zn-Al-LDHs prepared by the co-precipitation method. The corrosion potential can indicate the corrosion resistance of the zinc electrode, and the more negative is the corrosion potential, the easier is the corrosion of the electrode.

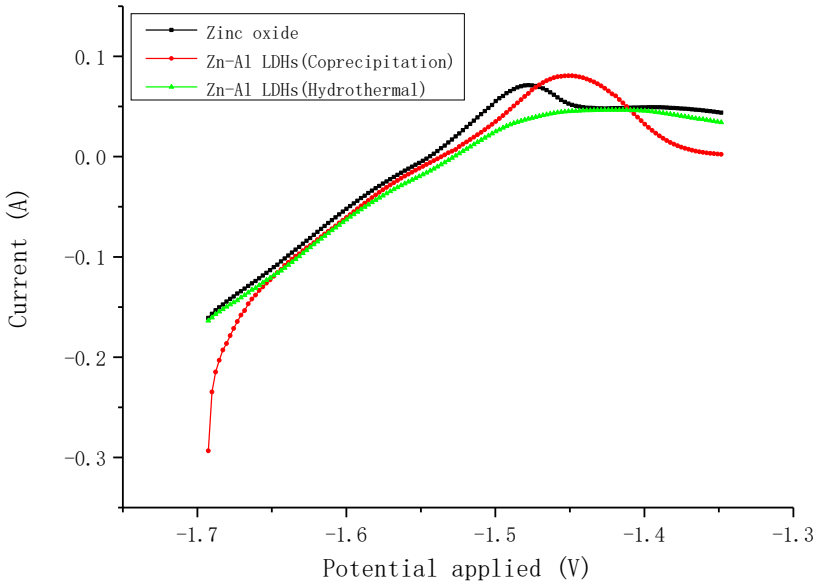

Figure 5. Potentiodynamic polarization curves of the Zn-Al-LDHs electrodes and the pure-ZnO electrode (Parameters: Scan range is -1.7V~-1.0V, Scan rate is 1 mv/s, auxiliary electrode is platinum electrode, reference electrode is calomel electrode, The frequency range is 0.01~10000 HZ, and the test temperature is room temperature.)

Table 2. Corrosion potential and corrosion current of the Zn-Al-LDHs electrodes and the pure-ZnO electrode (Parameters: scan range of -1.7~-1.0 V, scan rate of 1 mv/s, frequency range of 0.01~10000 HZ, and test temperature at room temperature, with the auxiliary electrode of a platinum electrode and the reference electrode of a calomel electrode)

Sample name	E_{corr}/ V	I_{corr}/ (mA·cm^{-2})	b_a (mV/dec)	b_c (mV/dec)
ZnO	-1.540	3.998	298.4	502.1
Zn-Al-LDHs by co-precipitation method	-1.536	3.719	435.5	659.2
Zn-Al-LDHs by hydrothermal method	-1.527	3.454	624.4	426.8

3.4 The galvanostatic charge/discharge curve analysis of different electrodes

The typical galvanostatic charge/discharge curves of zinc electrodes with Zn-Al-LDHs prepared by the hydrothermal method and the co-precipitation method and those of pure ZnO tested at the 20th cycle are shown in Fig. 6.

As shown in Fig. 6 (a), the charge platforms of pure ZnO and the Zn-Al-LDHs prepared by the hydrothermal method and the co-precipitation method appear at 1.95 V, 1.86 V, and 1.89 V, respectively, with the Zn-Al-LDHs electrodes having lower charge platforms. The decrease in the charge plateau voltage is an advantage of the suppression of H_2 formation, the improvement of the charge efficiency and the availability of cathode active materials. This means that Zn-Al-LDHs can improve the charge

efficiency mainly due to the low resistance of Zn-Al-LDHs, along with strong corrosion resistance and the promotion of charge transfer during reaction processes. Fig. 6 also shows that the charge platform of Zn-Al-LDHs prepared by the hydrothermal method is lower than that of Zn-Al-LDHs prepared by the co-precipitation method. By combining these results with those shown in Fig. 2 and Fig. 3, it can be found that the particle size, degree of dispersion and morphology of Zn-Al-LDHs affect the charging efficiency.

From Fig. 6 (b), the discharge platform of pure ZnO and the Zn-Al-LDHs prepared by the hydrothermal method and the co-precipitation method appear respectively at 1.67 V, 1.71 V, and 1.69 V. The increase in the discharge plateau is advantageous to the discharge capacity, the battery power and energy and the discharge performance. This means that the discharge platform of Zn-Al-LDHs is higher than that of ordinary zinc oxide and that it is a better Zn-Ni battery negative electrode material. Fig. 6 also shows that the discharge platform of Zn-Al-LDHs prepared by the hydrothermal method is higher than that of Zn-Al-LDHs prepared by the co-precipitation method. The particle size, degree of dispersion and morphology of Zn-Al-LDHs also affect the discharging efficiency. The smaller is the particle size and the better is the degree of dispersion, the better is the discharge performance.

We compared our results with those of similar works in the literature, and we found that in the 20th charge-discharge curves, the charging platform of the Zn-Al-LDHs electrode[22] in the literature is almost the same as that presented in this paper. However, as charging progressed, a second charging platform appeared in the Zn-Al-LDHs electrodes in the literature, reaching 1.95 V, which had a certain influence on the charging performance of the Zn-Ni battery. The Zn-Al-LDHs electrode prepared in this paper only showed a charging platform near 1.85 V, indicating that the charging performance of the Zn-Al-LDHs electrode prepared in this paper is better than that of others in the literature. In addition, the discharge platform of the Zn-Al-LDHs electrodes in the literature is less than 1.7 V, which is slightly inferior to the charging platform of the electrode prepared herein. Therefore, it can be seen that the performance of the Zn-Al-LDHs electrode prepared herein is superior to those in some studies.

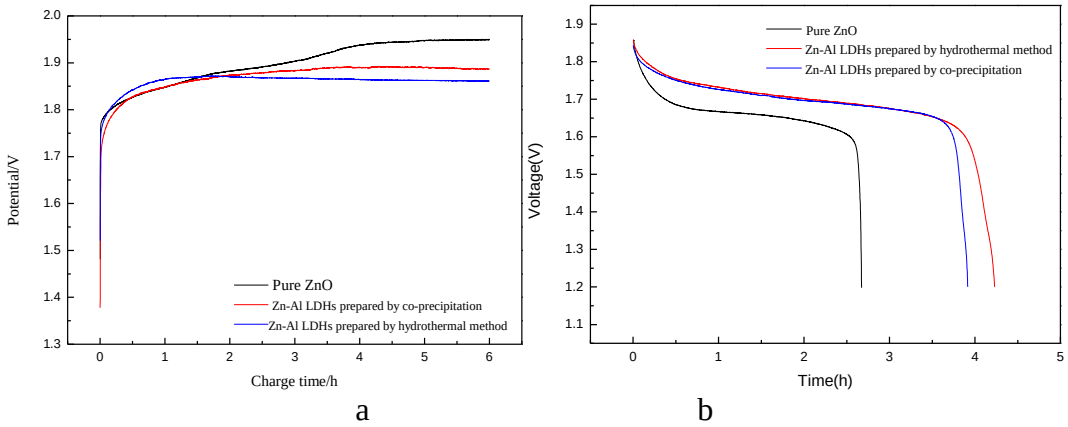

Figure 6. Zn-Al-LDHs and pure-ZnO electrodes 20th charge and discharge curves (charge and discharge system: 0.2 C charging for 6 h, 0.2 C discharging to 1.2 V)

3.5 The charge and discharge cycle curve analysis of different materials

Fig. 7 displays the variation of the discharge capacity with 40 cycles for the zinc electrodes prepared from pure ZnO and Zn-Al-LDHs (prepared by the hydrothermal method and the co-precipitation method) at current density of 0.2 C. It can be found in Fig. 7 that the discharge capacities of Zn-Al-LDHs electrodes prepared by the hydrothermal method and the co-precipitation method and that of pure-ZnO electrodes appear respectively at 519.4 $mAhg^{-1}$, 337 $mAhg^{-1}$ and 306 $mAhg^{-1}$ in the first cycle. The discharge capacity of Zn-Al-LDHs was lower than that of the pure-ZnO electrode, because compounds of zinc and aluminium reduce the discharge capacity, with the theoretical discharge capacities of 440 $mAhg^{-1}$ for Zn-Al-LDHs and 659 $mAhg^{-1}$ for ZnO. As shown in Fig. 7, the first discharge capacity was lower than that after a few cycles, mainly because the material of the zinc electrode had not been fully activated. The discharge capacities after 40 cycles of the Zn-Al-LDHs electrodes prepared by the hydrothermal and co-precipitation methods and the ordinary zinc oxide electrode were 354 $mAhg^{-1}$, 358.5 $mAhg^{-1}$ and 348 $mAhg^{-1}$, respectively, and the capacity retention ratios were 54%, 81.4%, and 79%, which showed that the Zn-Al-LDHs electrode has a higher capacity retention ratio and cycling stability than does the zinc oxide electrode. The lower resistance and better corrosion resistance made the charge transfer between particles easy to accelerate in the electrochemical reaction of the electrode, and the electrode has strong corrosion resistance, indicating that Zn-Al-LDHs has a higher capacity retention ratio and cycling stability and is more suitable for use as the active material in cathode materials of Ni Zn batteries. Fig. 7 also shows that the Zn-Al-LDHs electrode prepared by the hydrothermal method has a higher capacity retention ratio and cycling stability than that of the Zn-Al-LDHs electrode prepared by the co-precipitation method. Zn-Al-LDHs prepared by the hydrothermal method has fine particle size, a high degree of dispersion, regular morphology and thin thickness, which improved the charge and discharge performance and increased the cycling performance and stability.

Similarly, in the charge-discharge cycle curves, we also compared our results to those in the literature[22]. The capacity of the Zn-Al-LDHs electrode prepared in the literature is 400 $mAhg^{-1}$, which is close to the theoretical capacity of Zn-Al-LDHs (440 $mAhg^{-1}$). The Zn-Al-LDHs electrode prepared in this paper has a capacity of 337 $mAhg^{-1}$, and the previously published data is superior to that of the Zn-Al-LDHs electrode prepared in this paper. However, in the charge-discharge cycle, the cycle stability of the Zn-Al-LDHs electrode in the literature is not as described herein. Therefore, it can be seen from the results that the performance of the Zn-Al-LDHs electrode prepared herein is still superior to that of the Zn-Al-LDHs electrode prepared in some studies.

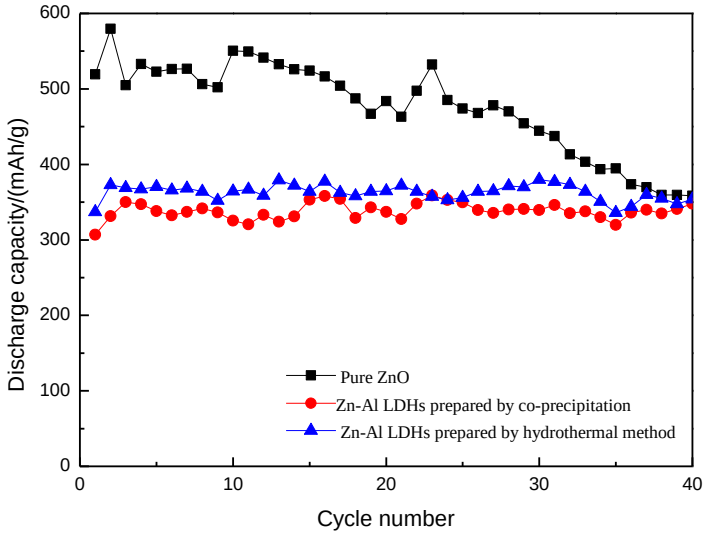

Figure 7. Charging and discharging cycles of Zn-Al-LDHs and ZnO electrodes (charge and discharge system: 0.2 C charging for 6 h, 0.2 C discharging to 1.2 V)

4. CONCLUSION

Through XRD, SEM and particle size analysis, Zn-Al-LDHs prepared by the hydrothermal method were found to have better crystallinity, regular morphology, uniform dispersion and smaller particle size, with d_{50}=12.47 μm.

The corrosion current densities of Zn-Al-LDHs prepared by the two methods were 4.646 mA·cm^{-2} and 4.851 mA·cm^{-2}, which were lower than that of ordinary zinc oxide (4.995 mA·cm^{-2}), illustrating that Zn-Al-LDHs has better corrosion resistance and lower charge-transfer impedance (Rct=21.8 Ω) than does ordinary zinc oxide.

The Zn-Al-LDHs electrode prepared by the hydrothermal method had a lower charge platform (1.68 V) and a higher discharge platform (1.71 V), with the retention ratio still 81.4% and the cycle efficiency reaching 90%. The comprehensive performance of this electrode was the best, and the material is more suitable as the active material of anode materials for zinc nickel batteries than is ordinary zinc oxide.

ACKNOWLEDGEMENTS
This work was supported by the National Natural Science Foundation of China (NO. 51774160) and the Opening foundation of the
State Key Laboratory of Pressure Hydrometallurgical Technology of Associated Non-Ferrous Metal Resources (NO. yy2016003).

References

1. W. Zhang, *J. Power Sources*, 66(1997)15-25.
2. X. Zhu, H. Yang and X. Ai, *J. Appl. Electrochem.*, 33(2003)607-612.
3. C. Cache, *Electrochim. Acta,* 138(1991)678-687.
4. J. Huang, Z. Yang, X. Xie, Z. Feng and Z. Zhang, *J. Power Sources,* 289(2015)8-16.
5. S. Xu, C. Yang, B. Zhang and H. Lei, *J. Power Sources,* 33(2009)985-988.

6. M. Yano, S. Fujitani, K. Nishio, Y. Akai and M. Kurimura, *J. Power Sources*, 74(1998)129-134.
7. T.Z. Palagyi, *J. Electrochem. Soc*., 108(1961)201-203.
8. H. Huan, Z. Yang and B. Yang, *J. Power Sources,* 271(2014)143-151.
9. Z. Yang, S. Wang and L. Zeng, *Mater.Chem.Phys.,* 39(2008)918-922.
10. S. Wang, Z. Yang, S, Shen and L. Zeng, *Chem.Res.Chin.Univ*., 27(2001)219-238.
11. W. Long , Z. Yang, X. Fan, B. Yang, Z. Zhao and J. Jing, *Electrochim. Acta,* 20(2009)64-68.
12. L. Zhu, H. Zhang and W. Li, *J. Phys. Chem. Solids,* 70(2009)45-54.
13. B. Yang, Z. Yang and R. Wang, *J. Power Sources,* 251 (2014)14-19.
14. R. Wang, Z. Yang, B. Yang, X. Fan and T. Wang, *J. Power Sources*, 246(2014)313-321.
15. X. Fan, Z. Yang, R. Wen, B. Yang and W. Long, *J. Power Sources,*224 (2013)80-85.
16. D. Jin, L. Yue and Z. Xu, *Wuji Huaxue Xuebao*, 21(2005)265-269.
17. X. Xie, Z. Yang and Z. Feng, *Electrochim. Acta*, 149(2014)101-107.
18. K. Wang, B. Yue and J. Zhu, *J. Inorg. chem*., 49(2017)33-37.
19. G. Liu, J. Zhou, Y. Wang and Z. Liu, *J. Surf. Eng.*, 46(2017)223-228.
20. L. Wang, S. Ge, Q. Shao, J. Li and L. Du, *J. Inorg. Chem.*, 32(2016)1896-1904.
21. L. Liu and Z. Yang, *Ionics,* 4(2018)1-11.
22. X. Fan , Z. Yang , W. Long , Z. Zhao and B. Yang , *J. Power Sources*, 92(2013)365-370.
23. Z. Feng, Z. Yang, B. Yang and Z. Zhang, *J. Power Sources,* 266(2014)22-28.